Article

Not peer-reviewed version

Effect of Carbon Dioxide Injection on Limestone Permeability Damage Induced by Alumina Nanoparticles for Enhanced Oil Recovery Applications

Ragheed Alali *, Kazunori Abe *, Khawaja Naweed Seddiqi , Hikari Fujii

Posted Date: 7 June 2023

doi: 10.20944/preprints202306.0509.v1

Keywords: nanoparticles enhanced oil recovery; pH control; alumina nanoparticles; permeability damage; transportability and retention

Article

Effect of Carbon Dioxide Injection on Limestone Permeability Damage Induced by Alumina Nanoparticles for Enhanced Oil Recovery Applications

Ragheed Alali [1,*], Kazunori Abe [1,*] Khawaja Naweed Seddiqi [2] and Hikari Fujii [1]

[1] Department of Earth Resource Engineering and Environmental Science, Graduate School of International Resource Sciences, Akita University, 1–1 Tegata Gakuen-Machi, Akita 010-8502, Japan; fujii@mine.akita-u.ac.jp

[2] Centre for Regional Revitalization in Research and Education, Akita University, 1–1 Tegata Gakuen-Machi, Akita 010-8502, Japan; naweed.cedeqe@gmail.com

* Correspondence: ragheedalali@hotmail.com; abe@mine.akita-u.ac.jp

Abstract: Enhanced oil recovery using nanoparticles is a promising method. However, when injected into a reservoir, nanoparticles can block pores and cause permeability damage. Therefore, enhancing their performance to lower the permeability damage effect is crucial. This study investigated the effect of pH alteration through carbon dioxide (CO_2) injection on the permeability damage of limestone caused by the aluminum oxide (α-Al_2O_3) nanofluid. The methodology involved nanofluid alternating CO_2 core flooding experiments by using nanofluids with pH of 4.5 and 2.8. After core flooding, permeability damage was calculated as a percentage of the reduction of the original permeability. The results revealed that the permeability damage in the case of nanofluid alternating CO_2 injection was 23.23%. In only nanofluid with a pH of 4.5 injection case, permeability damage was 47.53%. In the 2.8 pH nanofluid injection case, permeability damage was 31.01%. The retention of nanoparticles was confirmed through scanning electron microscopy and energy dispersive X-ray analysis. Permeability damage could be attributed to a large nanoparticles' agglomeration size, roughness of pore surfaces, and nanoparticle sedimentation. The results of the study revealed that altering pH through the α-Al_2O_3 nanofluid alternating CO_2 injection can effectively reduce the permeability damage of limestone.

Keywords: nanoparticles enhanced oil recovery; pH control; alumina nanoparticles; permeability damage; transportability and retention

1. Introduction

Oil remains a valuable energy resource worldwide. Since the fifties of the twentieth century, oil has been the lifeblood of many industries and will continue to be so for the foreseeable future. In the International Energy Outlook of 2021, the U.S. Energy Information Administration stated that the world's liquid fuel consumption is expected to increase by nearly 50% by 2050 [1]. The rise in energy consumption necessitates maximization of oil production from available reservoirs. Therefore, enhanced oil recovery is a critical topic of research.

Nanofluids are nanoscale colloidal solutions prepared by dispersing nanoparticles (solid phase) in a base fluid (liquid phase) [2]. Using nanoparticles for enhanced oil recovery is an economically viable [3] and promising method that has proven its potential in laboratory experiments [4–6]. One of the major advantages of nanoparticles enhanced oil recovery is the multitude of mechanisms involved in the recovery process. These mechanisms include wettability alteration [6–9], interfacial tension reduction [10,11], disjoining pressure [12–14], and pore plugging [14,15]. However, applying this method on a large scale remains challenging because of its immaturity compared with other enhanced oil recovery methods, environmental effects of this method, and performance uncertainty in large-scale reservoirs [16]. Improving the performance uncertainty issue requires maximizing the

 doi:10.20944/preprints202306.0509.v1

performance of nanoparticles for enhanced oil recovery. Several factors, such as nanofluid stability [14], nanoparticles type, and its compatibility with the reservoir's type and conditions, affect the performance of nanoparticles during enhanced oil recovery. [16,17].

After nanofluid injection in the reservoir, nanoparticles can get retained in the rock's pore space, close pore channels, and cause permeability damage [10,11,14,15,17,18]. Permeability damage is typically expressed as a percentage of reduction from the rock's original permeability (before nanofluid injection). Permeability damage indicates poor performance for the nanoparticles enhanced oil recovery, and pH control is typically used to enhance nanofluid performance [16].

Nanoparticle retention typically occurs through three mechanisms during the nanofluid injection process [19]. First, the sedimentation of nanoparticles resulting from instability [2,19]. Second, physical entrapment (filtration), which occurs when nanoparticles are larger than some of the pore throats or when the surface of the pores exhibits a rough geometry [2,10,19]. Third, the adsorption of nanoparticles onto the rock surface when the total potential energy between the nanoparticles and the rock surface is attractive [2,19]. Some retention of nanoparticles can be beneficial for diverting the flow of injected fluids toward unproduced oil and for altering the wettability of the rock surface. However, too much retention can be counterintuitive, detrimental to the efficiency of nanofluids, and could impede the oil recovery process [14,15].

Altering the pH of both the nanofluid, and the medium it is injected into changes stability and total interaction energy between the nanoparticles and the rock surface [2,20]. The stability of the nanofluid refers to the nanofluid's resistance to agglomeration and sedimentation. Therefore, more stable nanofluids exhibit superior performance. Stability can be explained using the Derjaguin, Landau, Verwey, and Overbeek (DLVO) theory. According to this theory, gravity and buoyancy forces are ignored, and the stability of the nanofluid depends only on the total interaction energy between nanoparticles. The total energy is the sum of Van der Waals attractive force and electrical double layer repulsive force [2]. Numerous factors, including nanoparticles' size and concentration, the dielectric constant of the base fluid, and zeta potential of the nanoparticles affect the total potential energy between the nanoparticles [2,20] and affect nanofluid stability.

The pH value of the nanofluid and its zeta potential are correlated [2,21]. When a material is submerged in an electrolyte solution, it is usually charged because of the adsorption of ions on the material's surface, or ionization of dissociable surface groups. Ions that determine the material's surface charge are called potential-determining ions or PDIs [21]. As mentioned, the zeta potential affects the total interaction energy and causes the pH control method to affect the performance of nanofluids and permeability damage.

The pH condition for less retention and permeability damage should satisfy the following two conditions:

- The pH value is far from the point of zero-charge, so the corresponding zeta potentials of nanoparticles and rock surface are high. When the pH value is at or near the point of zero-charge, the nanofluid loses its stability because of the weak repulsive force [8].
- The pH value is higher or lower than the point of zero-charge so that the signs of zeta potentials of nanoparticles and rock surface match each other.

Not satisfying these conditions eventually results in an attractive total potential energy that results in low nanofluid stability and high adsorption of nanoparticles on the rock surface.

A large number of research studies related to using nanoparticles in the oil and gas industry have focused on silicon dioxide (SiO_2) nanoparticles [4,5]. However, other types of commercially available nanoparticles have promising potentials. Among these types is aluminum oxide (Al_2O_3) nanoparticles, which have proven to be effective for enhanced oil recovery applications [5,6,10]. However, similar to the other types of nanoparticles, Al_2O_3 nanoparticles tend to cause permeability damage. In the case of Al_2O_3 nanoparticles, changing the pH of the base fluid (increasing or decreasing the concentration of H^+ ions) changes the surface charge and zeta potential, as displayed in Figure 1 [22], which changes stability and interaction energy between Al_2O_3 nanoparticles and the rock surface.

Preprints.org (www.preprints.org) | NOT PEER-REVIEWED | Posted: 7 June 2023 doi:10.20944/preprints202306.0509.v1

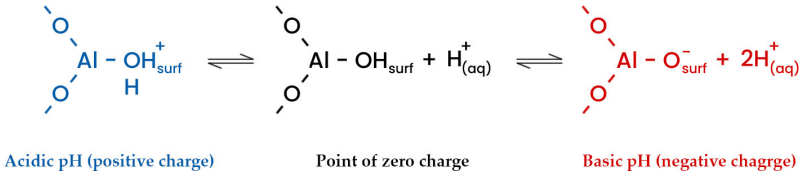

Figure 1. Surface charge of alumina in the aqueous solution at various pH conditions [22].

This study experimentally investigated the efficiency of the pH control method for reducing the permeability damage caused by the injection of Al_2O_3 nanofluids. The study involved performing core flooding experiments at various pH conditions and comparing permeability damage results. DLVO theory calculations, scanning electron microscopy (SEM), and energy dispersive X-ray (EDX) analysis were performed to confirm and evaluate nanoparticle retention. Limestone was used in the study because according to a study by Bayat et al., the positive surface potential of limestone renders it compatible with the positively charged Al_2O_3 nanoparticles [10].

2. Materials and Methods

2.1. Materials

Nanoparticles used in the experiments were alpha alumina nanoparticles (α-Al_2O_3), manufactured by SkySpring Nanomaterials with an average particle diameter of 50 nm. Limestone cores were bought from Kocurek Industries, Inc. Each core's diameter was approximately 1 inch, and its length was approximately 2 inches. The cores consisted of 97% calcite and 3% montmorillonite. Permeabilities and porosities of the cores were measured using the PoroPerm gas permeameter apparatus manufactured by Vinci Technologies. The properties of the three cores used in the core flooding experiments are mentioned in Table 1. Two more limestone cores were used for contact angle measurement and the initial pore surface evaluation.

When mixed with water, carbon dioxide (CO_2) dissolves and produces carbonic acid (H_2CO_3), which reduces the pH of the medium [23]. The same effect applies to nanofluids having water as their base fluid. Generally, the pH of formation water within limestone rocks is slightly basic [24]. Therefore, nanofluid alternating CO_2 injection was used to lower pH within limestone cores.

Table 1. Dimensions and measured properties of limestone cores used for core flooding.

Core ID	Diameter (mm)	Length (mm)	Gas Permeability (mD)	Porosity (%)
IDLS_1	25.52	50.78	229.444	17.38
IDLS_2	25.33	50.78	212.025	17.21
IDLS_3	25.27	50.82	208.178	16.93

2.2. Nanofluid Preparation and Properties

The nanofluid was prepared by dispersing α-Al_2O_3 nanoparticles in low salinity water base fluid with 1000 ppm sodium chloride (NaCl). The ball milling method using 2-mm zirconia beads was used to disperse nanoparticles. The weight of beads to weight of nanofluid ratio was 2.3, and ball milling was conducted at 200 rpm for 4 h. Hydrochloric acid (HCl) was added to the nanofluid to alter pH, and Cetrimonium bromide (CTAB) surfactant was added for enhanced stability [25]. The longest stability for the nanofluid was achieved at a pH of 4.5. The concentrations of materials required to prepare the nanofluid at pH value of 4.5 are mentioned in Table 2.

Zeta potential and nanoparticles' cluster size were measured using the dynamic laser light scattering apparatus ELSZ-1000ZS by Otsuka Electronics. The opaque appearance of the nanofluid

 doi:10.20944/preprints202306.0509.v1

allowed stability assessment through simple sedimentation tests. Finally, pH measurements were performed using a TPX-999i pH Meter manufactured by Toko Chemical Laboratories Co., Ltd.

Table 2. Concentrations of each material added to distilled water to prepare the α-Al_2O_3 nanofluid with a pH value of 4.5.

Material	Concentration (wt%)
α-Al_2O_3 nanoparticles	0.1
NaCl salt	0.1
Concentrated HCl acid	0.007
CTAB surfactant	0.03

2.3. Contact Angle Measurement

To measure the effects of the α-Al_2O_3 nanofluid on the wettability of limestone, the contact angle measurement test was conducted using the sessile drop method. One measurement was taken with the oil-saturated core submerged in 3.5 wt% NaCl brine. Next, the limestone core was submerged in nanofluid for 1 day, and the contact angle measurement was performed again in the same manner.

2.4. Core Flooding Experiments

Limestone cores were saturated with 3.5 wt% NaCl brine. Brine saturation was performed in an acrylic vacuum chamber. The cores were then saturated with crude oil using SRP 350 core flooding apparatus by Vinci Technologies displayed in Figure 2. The oil saturation process consisted of injecting the oil at a progressively increasing rate for 20 h. After oil saturation, the cores were aged in oil at 60 °C for at least 14 days. The oil's API gravity was 35.0. At 22 °C, oil had a density of 0.86 g/cm^3 and a viscosity of 7.70 cp.

Core flooding experiments were performed using the same core flooding apparatus displayed in Figure 2. Three core flooding experiments were conducted, and each of the experiments had three steps: the first step was low salinity water (LSW) injection. The second step was either nanofluid alternating CO_2 injection or only nanofluid injection. The final step was the injection of five pore volumes (PVs) of the sweeping fluid, which was LSW with CTAB surfactant and had a pH value of 4.5. The sweeping fluid was prepared to maintain the same surface charge for the pore surface and the nanoparticles remaining in the pores during the sweeping step. Each of the first two steps lasted until no oil was produced for two consecutive PVs.

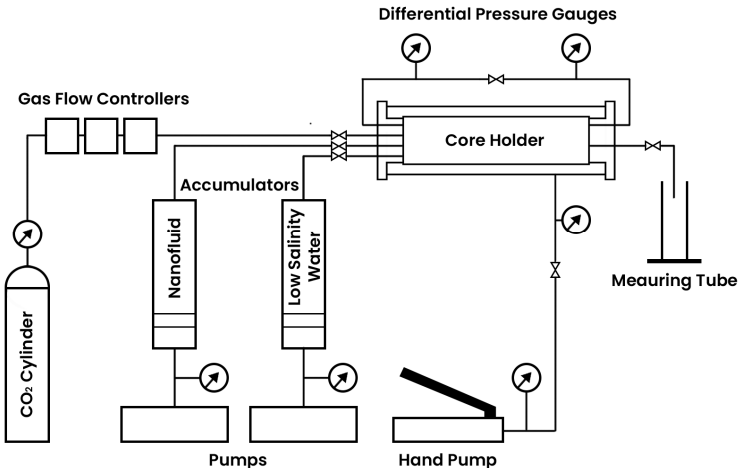

Figure 2. Schematic of the SRP 350 core flooding apparatus by Vinci Technologies.

The first core flooding experiment (IDLS_1) was LSW injection followed by nanofluid alternating CO_2, the ratio was 1 PV of nanofluid to 6 PVs of the CO_2, which was selected after some experimentation that was effective in achieving and maintaining a low pH value over a long period,

Preprints.org (www.preprints.org) | NOT PEER-REVIEWED | Posted: 7 June 2023 doi:10.20944/preprints202306.0509.v1

as illustrated in Figure 3. In the second core flooding experiment (IDLS_2), after LSW injection, only the α-Al_2O_3 nanofluid was injected. The final core flooding experiment (IDLS_3) was the same as the second experiment, except, the amount of HCl in the nanofluid was doubled to investigate the effect of high HCl concentration on pH alteration and permeability damage results. The nanofluid in the third core flooding experiment had a pH of 2.8 instead of 4.5.

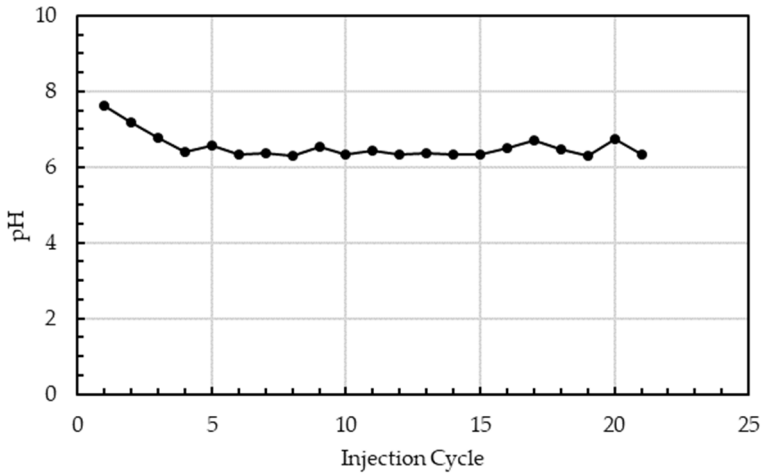

Figure 3. pH of the effluent during nanofluid alternating CO_2 injection after each injection cycle.

2.5. Permeability Damage Evaluation

After each core flooding experiment, the core was cleaned with toluene and methanol by using a Soxhlet extractor for 3 days each, and subsequently dried in a vacuum oven for 1 day. Next, the post flooding permeability was measured again using the PoroPerm gas permeameter apparatus. Finally, the IDLS_2 core was sliced into 30-µm sections after the core flooding experiment. Thin sections were carbon coated, and then a scanning electron microscope manufactured by InTouchScope™ was used to investigate nanoparticles' retention and pore surface roughness. IDLS_2 core exhibited the highest permeability damage after post flooding permeability measurements; therefore, the model was selected for SEM analysis. Observing the nanoparticles using SEM images was performed manually, and IDLS_2 core provided an excellent chance of locating the retained nanoparticles within the pores.

3. Results and Discussion

3.1. Zeta Potential and Stability

The zeta potential measurements of α-Al_2O_3 nanoparticles in the nanofluid are displayed in Figure 4a. According to the DLVO theory, higher zeta potential results in higher repulsion between nanoparticles. Therefore, the nanofluid exhibits high stability. The dimensionless total potential energy of the interaction between the nanoparticles was calculated using equations 1 to 4 [2,26], and the results are presented in Figure 4b.

$$V_T = V_{VDW} + V_{EDL} \quad (1)$$

$$V_{VDW} = -\frac{A}{6h}\left[\frac{a_p^2}{2a_p}\right] \quad (2)$$

$$V_{EDL} = 4\pi\varepsilon_r\varepsilon_0 a_p \zeta_p^2 \left(\frac{a_p + h}{2a_p + h}\right) ln\left[1 + \frac{a_p}{a_p + h} exp(-\kappa h)\right] \quad (3)$$

 doi:10.20944/preprints202306.0509.v1

$$V_{TD}=\frac{V_T}{k_B T} \quad (4)$$

where V_T, V_{VDW}, V_{EDL}, and V_{TD} are the total energy of interaction, Van der Waals attractive force, electrical double layer repulsive force, and the dimensionless total energy of interaction, respectively, A is the Hamaker constant for Al_2O_3 nanoparticle–nanoparticle interaction (5.3×10^{-20}) [17], h is the separation distance between nanoparticles (m), a_p is nanoparticle's radius (m), ε_r is the relative dielectric constant of the base fluid (78.5 for water) [17], ε_0 is the permittivity of the free space (8.85×10^{-12} C/V/m), ζ_p is the zeta potential of nanoparticles (mV), k_B is the Boltzmann constant (1.3805×10^{-23} J/°K) [17], T is the temperature of the system (295 °K), and $???$ is the Debye reciprocal length (m^{-1}).

The nanoparticles had the highest zeta potential at a pH value of 4.5. DLVO calculations revealed that the interaction between nanoparticles was repulsive in all cases. However, a notable increase in nanoparticles' repulsion occurred when pH was decreased and zeta potential increased. These results are reflected in Figure 5, where a sedimentation test at 4.5, 6.7, and 7.5 pH conditions revealed the same trend. The highest stability was achieved at a pH of 4.5.

Because of the relation between Van der Waals attractive force and the distance between the nanoparticles, when nanoparticles collide with each other, they form clusters that are inseparable unless subjected to strong agitation. This clustering behavior is detrimental to nanofluid stability. According to DLVO theory, the electrical double layer force is the only force acting against the clustering of nanoparticles. The electrical double layer force had a positive correlation with zeta potential, which increased at lower pH conditions, explaining the stability results.

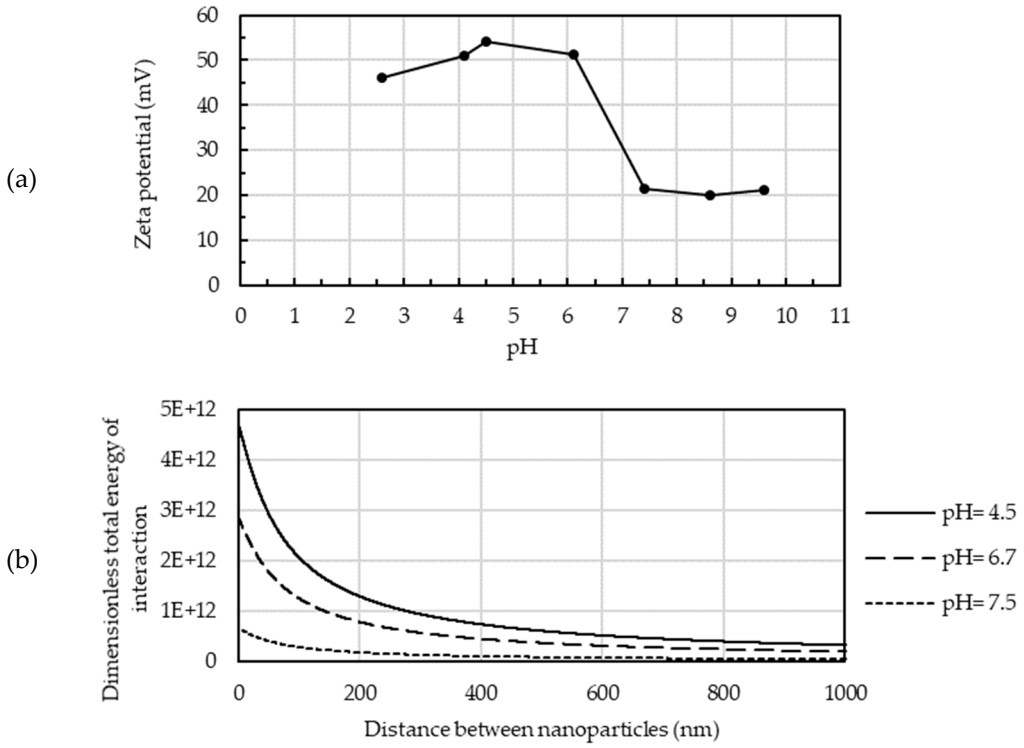

Figure 4. (a) Zeta potential of α-Al_2O_3 nanoparticles at various pH values. **(b)** The dimensionless total energy of interaction between nanoparticles in relation to the distance between nanoparticles at various pH values.

Preprints.org (www.preprints.org) | NOT PEER-REVIEWED | Posted: 7 June 2023 doi:10.20944/preprints202306.0509.v1

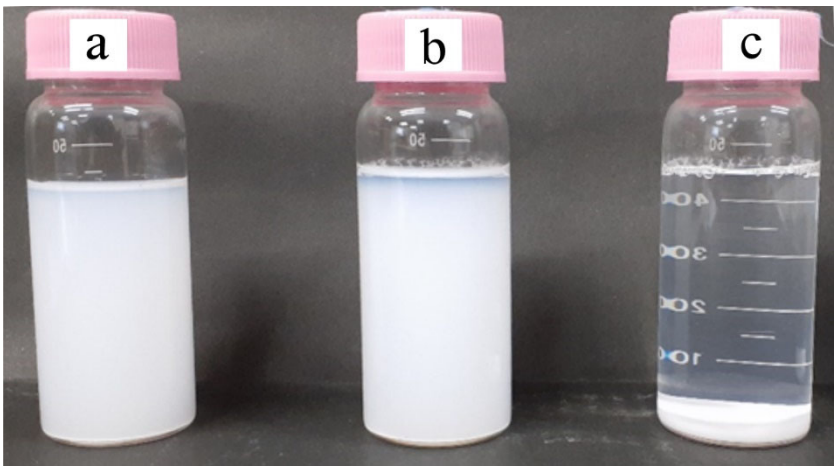

Figure 5. Sedimentation of nanoparticles after 24 h of nanofluid preparation at various pH conditions. (a) pH = 4.5, (b) pH = 6.7, and (c) pH = 7.5.

3.2. Limestone Permeability Damage

pH within the limestone core was assumed to be the average of all effluents' pH values. In all cases, the pH of the effluent was measured immediately after the injection of each pore volume to avoid equilibrium between the dissolved CO_2 and air. After conducting the core flooding experiments, cleaning the cores, and measuring the new permeability of each core, permeability damage was calculated as the permeability's reduction percentage. The permeability damage and pH results are presented in Table 3.

Table 3. Permeability damage to the limestone cores after each core flooding experiment.

Experiment's Description	Effluent's Average pH	Original Gas Permeability (mD)	Post Flooding Gas Permeability (MD)	Permeability Reduction Percentage
Nanofluid alternating CO_2 injection	6.5	229.444	176.14	23.23 %
Nanofluid injection	7.6	212.025	111.23	47.54 %
Low-pH nanofluid injection	7.2	208.178	143.61	31.02 %

The total interaction energy between nanoparticles and the rock surface was calculated according to DLVO theory using equations 1, and 4 to 7. In this case, the equations of V_{VDW} and V_{EDL} differ considerably because of the interaction being a sphere-plate interaction instead of a sphere-sphere interaction as in the case of nanoparticles' interactions [20]. The results are presented in Figure 6.

$$V_{VDW} = -\frac{A}{6}\left[\frac{2(1+H)}{H(2+H)} + ln\left(\frac{H}{2+H}\right)\right] \quad (5)$$

$$H = \frac{h}{a_p} \quad (6)$$

$$V_{EDL} = \left(\frac{\varepsilon_r \varepsilon_0 a_p}{4}\right)\left[2\zeta_1\zeta_2\, ln\left(\frac{1+exp(-\kappa h)}{1-exp(-\kappa h)}\right) + \left(\zeta_1^2+\zeta_2^2\right) ln(1-exp(-2\kappa h))\right] \quad (7)$$

where ζ_1 and ζ_2 are the zeta potentials of the nanoparticles and the rock surface, respectively (mV).

 doi:10.20944/preprints202306.0509.v1

The results revealed that permeability reduction occurred in all cases. However, the nanofluid alternating CO_2 injection case resulted in the least permeability damage. As displayed in Figures 4–6, lower pH conditions resulted in stronger repulsion between the nanoparticles themselves, and between nanoparticles and the rock surface. The stronger repulsion in those cases resulted in less retention of nanoparticles because sedimentation and adsorption are two of the main nanoparticles' retention mechanisms. Therefore, the lower permeability damage when nanofluid was alternately injected with the CO_2 was attributed to the lower pH condition within the core.

Despite the lower pH condition in the nanofluid alternating CO_2 injection core flooding experiment (IDLS_1), it was not sufficient to completely prevent the continuous accumulation of nanoparticles after injection into each pore volume of nanofluid. In all experiments, the differential pressure increased during the nanofluid injection step, as displayed in Figure 7. This increase proved that the pore-plugging effect occurred in all experiments. Nevertheless, in the nanofluid alternating CO_2 injection experiment, the plugging effect occurred at a slower rate. This conclusion was based on the slower rise in the differential pressure compared with those in other experiments.

In the second core flooding experiment (IDLS_2), the nanofluid was injected without alternating gas, the pH value within the core was high. This phenomenon resulted in unstable nanofluid and weak repulsion between the nanoparticles and the rock surface. Eventually, permeability damage was the highest.

In the final core flooding experiment (IDLS_3), the low-pH nanofluid had a pH value of 2.8 after increasing the concentration of the hydrochloric acid. The dissolution of calcite was proportional to the concentration of H^+ at pH values lower than 4 in aqueous solutions [27]. Therefore, lowering the pH of the water-based nanofluid resulted in a higher dissolution of calcite, which not only increased the pH within the core but also resulted in an increased amount of calcium chloride ($CaCl_2$). A higher concentration of $CaCl_2$ is detrimental to the stability of α-Al_2O_3 nanoparticles because the increased concentration of Cl^- anions bridge the positively charged alumina nanoparticles. This effect creates larger nanoparticle clusters and lowers nanofluid stability [28]. However, the higher dissolution of calcite was not completely negative in the low-pH nanofluid injection experiment because it mitigated some permeability damage of nanoparticles' sedimentation.

(a)

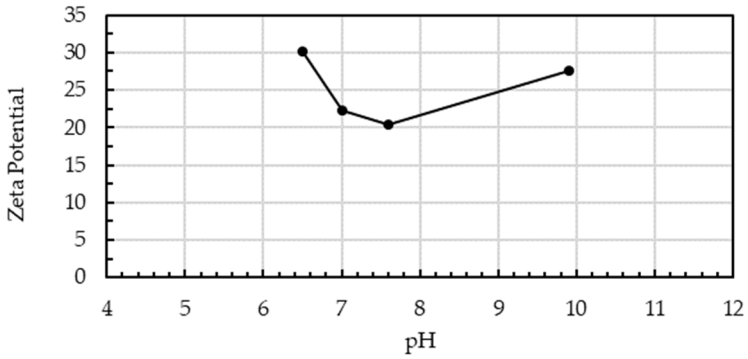

(b)

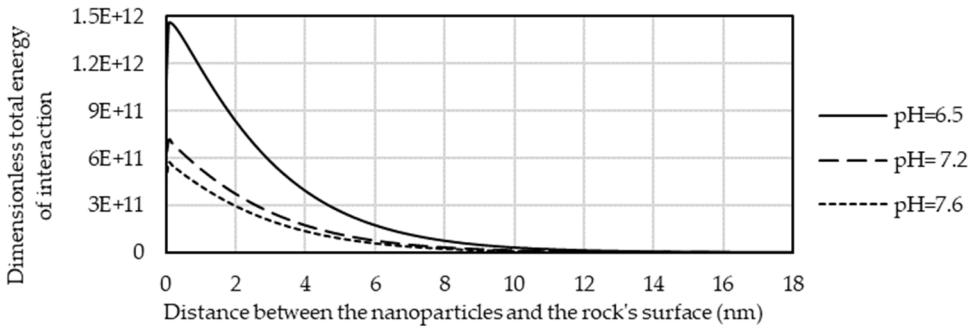

 doi:10.20944/preprints202306.0509.v1

Figure 6. (a) Zeta potential of limestone powder in 0.1 wt% NaCl water and 0.03 wt% CTAB surfactant at various pH values. **(b)** The dimensionless total energy of interaction between α-Al_2O_3 nanoparticles and limestone rock surface in relation to the distance between them at various pH values.

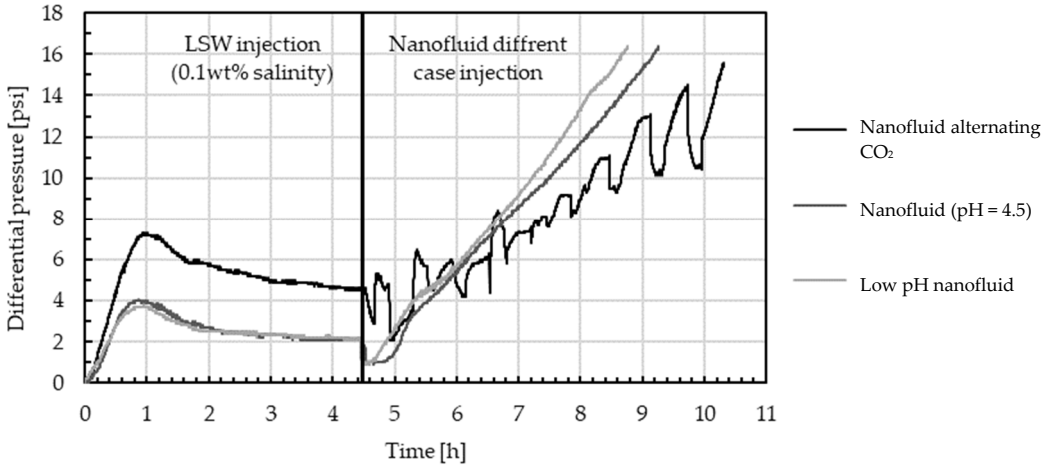

Figure 7. Differential pressure between the core's inlet and outlet during LSW injection and nanofluid injection steps.

3.3. Permeability Damage Mechanisms

Permeability damage was high in all cases regardless of the pH value. Investigation of the causes revealed the following conclusions:

- Although the nanofluid was stable in the low-pH case, some sedimentation of nanoparticles occurred, but not as much as in the other experiments in which sedimentation was high. In all experiments, sedimentation contributed to the retention of nanoparticles inside cores.
- The average cluster size of the nanoparticles at a pH of 4.5 was approximately 250 nm, and at a pH of 2.8, the average cluster size was 290 nm. The smallest size was 250 nm and was achieved using the ball milling method. However, the size was not sufficiently small to not cause permeability damage. The pore size distribution of a limestone core similar to the cores used in the experiments was used to obtain an approximate difference between the pore size and the nanoparticles' size. As depicted in Figure 8, approximately 20% of the pores were too small for the smallest nanoparticles, and another 5% of the pores were too small for 25% of the nanoparticles. This case excluded the agglomeration occurring inside the core during the injection process, which rendered the retention through straining more impactful on permeability.
- The roughness of the pore surface considerably influences the retention of nanoparticles inside the pores. The nanoparticles tend to get into the dents of the rough surface because of Brownian motion or repulsion between them. However, the repulsion between the nanoparticles and pore surface is only effective at a short distance, as displayed in Figure 6b, and that distance is shorter than the depth of the rough surface's dents. The surface roughness was investigated using SEM images, and the resulting images of the pores' surfaces are displayed in Figure 9. The images revealed that the surface of the pores was rough in general, but it had some smooth surfaces. Some pore channels were rough on one side and smooth on the other side.

 doi:10.20944/preprints202306.0509.v1

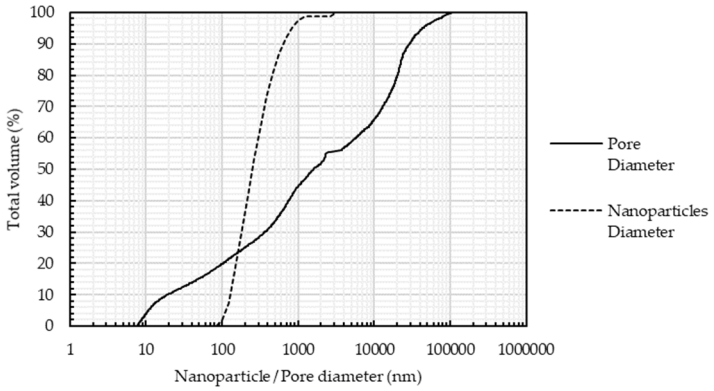

Figure 8. Size distributions of limestone pores and α-Al_2O_3 nanoparticles in the nanofluid at a pH value of 4.5.

The pores' surface was mostly covered with irregular bumps and dents, which hindered the flow of nanoparticles and resulted in higher retention and permeability damage to the core. This phenomenon was confirmed by obtaining SEM pictures and EDX analysis of a thin section from the inlet area of the IDLS_2 core after the core flooding experiment. Figure 10a displays the EDX analysis that confirmed the nanoparticles' retention in Figure 10b, and Figure 10c shows another example of retention within the rough dents of the limestone surface.

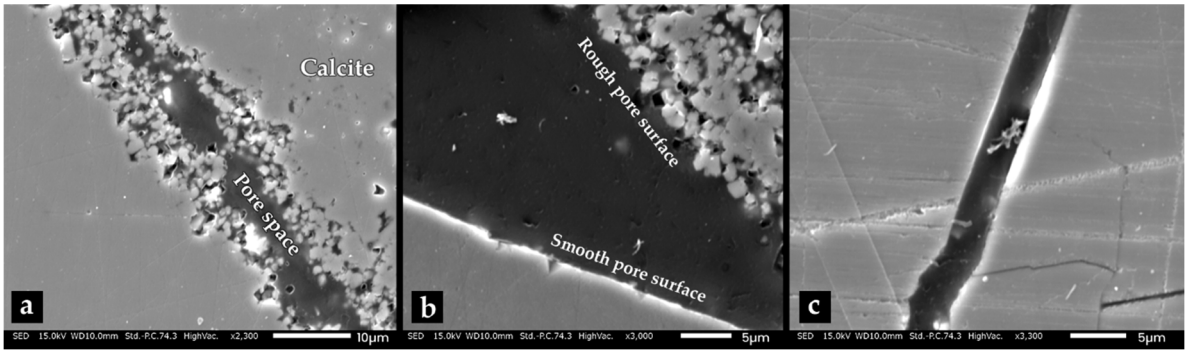

Figure 9. Scanning electron microscopy (SEM) images of an Indiana limestone sample. Light area: calcite; Dark area: pore space. Image **(a)** displays pore channels with a rough surface. Image **(b)** shows a channel with only one side being rough. Image **(c)** shows a smooth pore channel.

In addition to sedimentation, forms of the physical entrapment of nanoparticles are a major cause of permeability damage. The pH had a limited effect on these mechanisms, which caused all injection cases to have considerably high permeability damage, even at lower pH values. The result of this study indicated that altering pH through CO_2 gas injection positively affects permeability damage, but pH does not affect some retention mechanisms. Therefore, pH should be considered as one of several other factors that should be considered when using the α-Al_2O_3 nanofluid for enhanced oil recovery in limestones.

 doi:10.20944/preprints202306.0509.v1

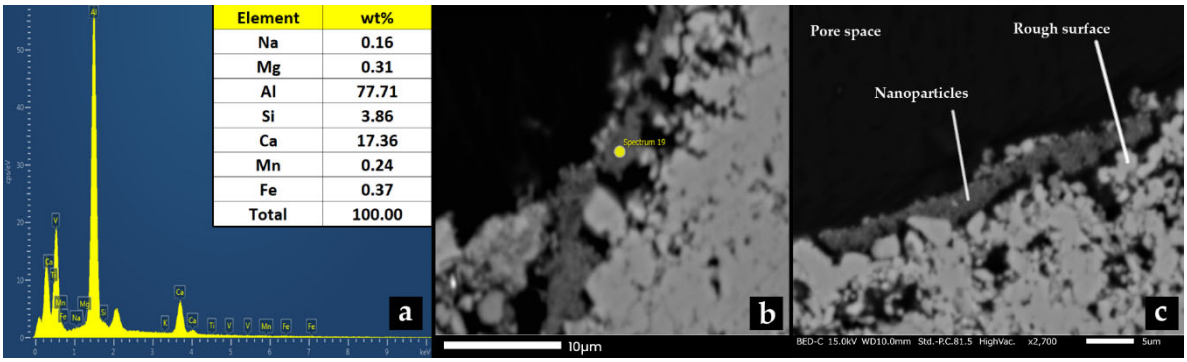

Figure 10. Observed nanoparticles inside the IDLS_2 core after the core flooding experiment. Image (a) displays EDX analysis confirming the presence of nanoparticles. Image (b) shows the spot where EDX analysis was performed. Image (c) shows another example of trapped nanoparticles in the dents of the pores' rough surface.

Oil Recovery

Oil recovery was slightly higher in the experiments that did not involve CO_2 injection, as displayed in Figure 11 and Table 4. Higher recovery occurred during the second and third steps of core flooding processes and could be attributed to pore blocking, disjoining pressure, wettability alteration, and interfacial tension reduction. The cores used in the experiments had high permeability. In such cases, the flow of the injected fluids tended to move from the inlet to the outlet through the widest channel. This phenomenon left oil droplets in the smaller pore channels unproduced, especially as the cores were oil wet. This phenomenon was observed at the end of the LSW flooding when the oil stopped being produced and the differential pressure almost stabilized as previously displayed in Figure 7.

Table 4. Oil recovery results of each experiment.

Experiment's Description	Oil Recovery Due to Low Salinity Water Injection (%)	Oil Recovery Due to Nanofluid and Sweeping Fluid Injections (%)	Overall Oil Recovery
Nanofluid alternating CO_2 injection	40.03	10.93	50.93
Nanofluid injection	38.79	14.13	52.92
Low-pH nanofluid injection	37.77	15.11	52.88

Preprints.org (www.preprints.org) | NOT PEER-REVIEWED | Posted: 7 June 2023 doi:10.20944/preprints202306.0509.v1

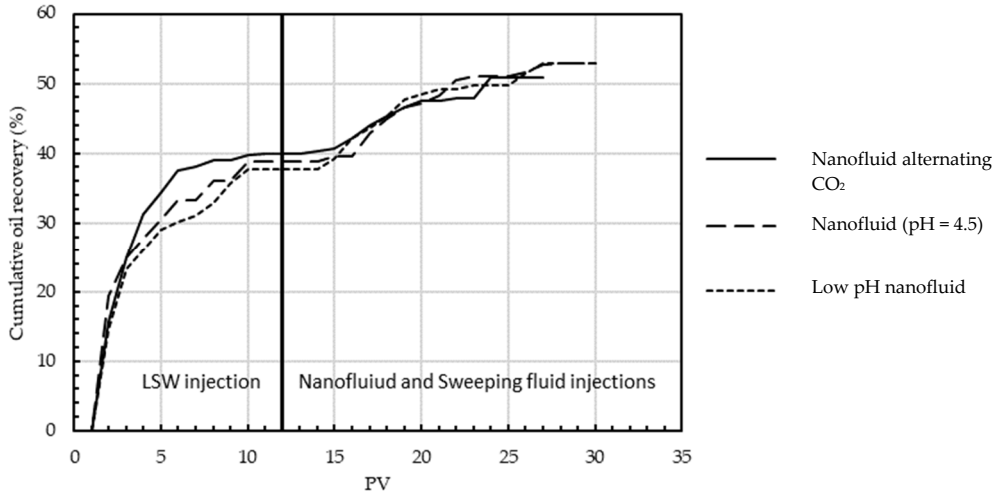

Figure 11. Cumulative oil recovery during all core flooding experiments.

When nanofluid injection was initiated, the pore-plugging effect of the nanoparticles occurred after a few PV, which caused the nanofluid to flow into the pores in which oil was trapped. This phenomenon was evident by the increase in the differential pressure and absence of oil in the effluent during the first few PV. The attachment and spreading of nanoparticles onto the pore surface allowed the nanoparticles to exert disjoining pressure on oil droplets, separating them from the rock surface. The attachment of nanoparticles also alters the wettability of the calcite from oil wet to intermediate wet. The wettability alteration test result is displayed in Figure 12, and it is consistent with the results of Bayat et al. [10]. Finally, interfacial tension reduction effectively increased oil recovery because of the presence of both CTAB surfactant and Al_2O_3 nanoparticles themselves.

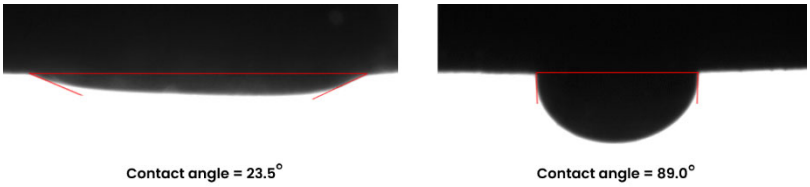

Figure 12. Difference in the contact angle before submerging in nanofluid (left) and after submerging in nanofluid (right) indicating wettability alteration.

In experiments with greater permeability damage, more nanoparticles were retained in the core, and more nanoparticles spread on the surface, which enhanced the pore plugging, disjoining pressure, and wettability alteration effects. Therefore, oil recovery was enhanced in the cases in which permeability damage was higher.

4. Conclusions

In this study, the effects of pH control using CO_2 on the retention of α-Al_2O_3 nanoparticles and limestone permeability damage were investigated. The results revealed that CO_2 gas injection with the α-Al_2O_3 nanofluid caused lower permeability damage to the limestone cores than cases that did not include CO_2 gas. This phenomenon could be attributed to the lower pH condition after the formation of H_2CO_3, which resulted in a stronger positive total energy of interaction between the nanoparticles themselves and between the nanoparticles and the rock surface. This phenomenon increased the stability of the nanofluid in the core and increased the repulsion between the nanoparticles and the rock surface, which reduced the retention of nanoparticles inside the core. The observed results were consistent with DLVO theory calculations. However, even at lower pH conditions, the permeability damage was not negligible because of sedimentation, agglomeration of particles of large size, and the rough pore geometry of the limestone samples.

Oil recovery results were lower in the nanofluid alternating CO_2 injection case than in only nanofluid injection cases because of the lower spreading of nanoparticles across the limestone surface and lower pore plugging, which are necessary for the enhanced oil recovery mechanisms of the nanofluid.

Author Contributions: writing—original draft preparation, R.A.; writing—review and editing, K.A and K.N.S.; supervision, K.A and H.F.; funding acquisition, K.A. All authors have read and agreed to the published version of the manuscript.

Funding: This research was funded by JSPS KAKENHI, grant number JP21K04959, and Akita University Support for Fostering Research Project.

Acknowledgments: The authors are grateful for Akita University for providing a professional research environment.

Conflicts of Interest: The authors declare no conflict of interest.

References

1. International Energy Outlook. Available online: https://www.eia.gov/outlooks/ieo/pdf/IEO2021_ReleasePresentation.pdf (Accessed on 20 January2021).
2. Chakraborty, S.; Panigrahi, P.K. Stability of nanofluid: a review. Appl Therm Eng 2020, 174, 115259. DOI: 10.1016/j.applthermaleng.2020.115259.
3. Ajulibe, D.; Ogolo, N.; Ikiensikimama, S. Viability of SiO2 nanoparticles for enhanced oil recovery in the Niger Delta: a comparative analysis. In Proceedings of the SPE Nigeria Annual International Conference and Exhibition, 2018. DOI: 10.2118/193423-MS.
4. Alsaba, M.T.; Al Dushaishi, M.F.; Abbas, A.K. A comprehensive review of nanoparticles applications in the oil and gas industry. J Petrol Explor Prod Technol 2020, 10, 1389–1399. DOI: 10.1007/s13202-019-00825-z.
5. Hogeweg, A.S.; Hincapie, R.E.; Foedisch, H.; Ganzer, L. Evaluation of aluminium oxide and titanium dioxide nanoparticles for EOR applications. In Proceedings of the SPE Europec Featured at 80th EAGE Conference and Exhibition, 2018. DOI: 10.2118/190872-MS.
6. Ogolo, N.A.; Olafuyi, O.A.; Onyekonwu, M.O. Enhanced oil recovery using nanoparticles. In Proceedings of the SPE Saudi Arabia Section Technical Symposium and Exhibition, 2012. DOI: 10.2118/160847-MS.
7. Al-Anssari, S.; Barifcani, A.; Wang, S.; Maxim, L.; Iglauer, S. Wettability alteration of oil-wet carbonate by silica nanofluid. J Colloid Interface Sci 2016, 461, 435–442. DOI: 10.1016/j.jcis.2015.09.051.
8. Li, S.; Torsæter, O. The impact of nanoparticles adsorption and transport on wettability alteration of water wet berea sandstone. In Proceedings of the SPE/IATMI Asia Pacific Oil & Gas Conference and Exhibition, 2015. DOI: 10.2118/176256-MS.
9. Neubauer, E.; Hincapie, R.E.; Borovina, A.; Biernat, M.; Clemens, T.; Ahmad, Y.K. Influence of nanofluids on wettability changes and interfacial tension reduction. In Proceedings of the SPE Europec, 2020. DOI: 10.2118/200643-MS.
10. Esfandyari Bayat, A.; Junin, R.; Samsuri, A.; Piroozian, A.; Hokmabadi, M. Impact of metal oxide nanoparticles on enhanced oil recovery from limestone media at several temperatures. Energy Fuels 2014, 28, 6255–6266. DOI: 10.1021/ef5013616.
11. Hendraningrat, L.; Li, S.; Torsaeter, O. A coreflood investigation of nanofluid enhanced oil recovery in low-medium permeability Berea sandstone. In Proceedings of the SPE International Symposium on Oilfield Chemistry, 2013. DOI: 10.2118/164106-MS.
12. Wasan, D.T.; Nikolov, A.D. Spreading of nanofluids on solids. Nature 2003, 423, 156-159. DOI: 10.1038/nature01591.
13. Chengara, A.; Nikolov, A.D.; Wasan, D.T.; Trokhymchuk, A.; Henderson, D. Spreading of nanofluids driven by the structural disjoining pressure gradient. J Colloid Interface Sci 2004, 280, 192–201. DOI: 10.1016/j.jcis.2004.07.005.
14. Ilyas, S.U.; Pendyala, R.; Marneni, N. Stability of nanofluids. Eng Appl Nanotechnol Energy Drug Deliv 2017, 1–31. DOI: 10.1007/978-3-319-29761-3_1.
15. Udoh, T.H. Improved insight on the application of nanoparticles in enhanced oil recovery process. Sci Afr 2021, 13, e00873. DOI: 10.1016/j.sciaf.2021.e00873.
16. Iravani, M.; Khalilnezhad, Z.; Khalilnezhad, A. A review on application of nanoparticles for EOR purposes: history and current challenges. J Petrol Explor Prod Technol 2023, 13, 959–994. DOI: 10.1007/s13202-022-01606-x.
17. Esfandyari Bayat, A.; Junin, R.; Shamshirband, S.; Tong Chong, W. Transport and retention of engineered Al2O3, TiO2 and SiO2 nanoparticles through various sedimentary rocks. Sci Rep 2015, 5, 1–12. DOI: 10.1038/srep14264.

18. Keykhosravi, A.; Bedrikovetsky, P.; Simjoo, M. Experimental insight into the silica nanoparticle transport in dolomite rocks: spotlight on DLVO theory and permeability impairment. J Petrol Sci Eng 2022, 209, 109830. DOI: 10.1016/j.petrol.2021.109830.
19. Emeka, O.J.; Ifeanyi, O.; Chikwe, A.; Nwachukwu, A.; Ndubuisi, O.; Ifeanyi, O.; Chidiebere, O.A. Effect of application of aluminium oxide on recovery in enhanced oil recovery. J Eng Appl Sci 2021, 6, 41–48.
20. Khilar, K.C.; Fogler, H.S. Migrations of Fines in Porous Media 12; Springer Science & Business Media, 1998.
21. Derkani, M.H.; Fletcher, A.J.; Fedorov, M.; Abdallah, W.; Sauerer, B.; Anderson, J.; Zhang, Z.J. Mechanisms of surface charge modification of carbonates in aqueous electrolyte solutions. Colloids Interfaces 2019, 3, 62. DOI: 10.3390/colloids3040062.
22. Kasprzyk-Hordern, B. Chemistry of alumina, reactions in aqueous solution and its application in water treatment. Adv Colloid Interface Sci 2004, 110, 19–48. DOI: 10.1016/j.cis.2004.02.002.
23. Peng, C.; Crawshaw, J.P.; Maitland, G.C.; Trusler, J.M.; Vega-Maza, D. The pH of CO2-saturated water at temperatures between 308 K and 423 K at pressures up to 15 MPa. J Supercrit Fluids 2013, 82, 129–137. DOI: 10.1016/j.supflu.2013.07.001.
24. Derkani, M.H.; Fletcher, A.J.; Abdallah, W.; Sauerer, B.; Anderson, J.; Zhang, Z.J. Low salinity waterflooding in carbonate reservoirs: review of interfacial mechanisms. Colloids Interfaces 2018, 2, 20. DOI: 10.3390/colloids2020020.
25. Cacua, K.; Ordoñez, F.; Zapata, C.; Herrera, B.; Pabón, E.; Buitrago-Sierra, R. Surfactant concentration and pH effects on the zeta potential values of alumina nanofluids to inspect stability. Colloids Surf A Physicochem Eng Aspects 2019, 583, 123960. DOI: 10.1016/j.colsurfa.2019.123960.
26. Nguyen, A.V.; Evans, G.M.; Jameson, G.J. Electrical double-layer interaction between spherical particles. In Encyclopedia of Surface and Colloid Science; CRC Press: Boca Raton, 2015; pp. 2017-2027.
27. Sjoeberg, E.L.; Rickard, D.T. Calcite dissolution kinetics: surface speciation and the origin of the variable pH dependence. Chem Geol 1984, 42, 119–136. DOI: 10.1016/0009-2541(84)90009-3.
28. Bayat, A.E.; Junin, R.; Ghadikolaei, F.D.; Piroozian, A. Transport and aggregation of Al 2 O 3 nanoparticles through saturated limestone under high ionic strength conditions: measurements and mechanisms. J Nanopart Res 2014, 16, 1–12.